

# Enhancement of the helium resonance lines in the solar atmosphere by suprathreshold electron excitation I: non-thermal transport of helium ions

G.R. Smith<sup>\*</sup>, C. Jordan

*Department of Physics (Theoretical Physics), Oxford University, 1 Keble Road, Oxford OX1 3NP, UK*

8 August 2002

## ABSTRACT

Models of the solar transition region made from lines other than those of helium cannot account for the strength of the helium lines. However, the collisional excitation rates of the helium resonance lines are unusually sensitive to the energy of the exciting electrons. Non-thermal motions in the transition region could drive slowly-ionizing helium ions rapidly through the steep temperature gradient, exposing them to excitation by electrons characteristic of higher temperatures than those describing their ionization state. We present the results of calculations which use a more physical representation of the lifetimes of the ground states of He I and He II than was adopted in earlier work on this process. New emission measure distributions are used to calculate the temperature variation with height. The results show that non-thermal motions can lead to enhancements of the He I and He II resonance line intensities by factors that are comparable with those required. Excitation by non-Maxwellian electron distributions would *reduce* the effects of non-thermal transport. The effects of non-thermal motions are more consistent with the observed spatial distribution of helium emission than are those of excitation by non-Maxwellian electron distributions alone. In particular, they account better for the observed line intensity ratio  $I(537.0 \text{ \AA})/I(584.3 \text{ \AA})$ , and its variation with location.

**Key words:** line: formation – Sun: atmospheric motions – Sun: transition region – Sun: UV radiation.

## 1 INTRODUCTION

The resonance lines of He I (at 584.3 Å) and He II (at 303.8 Å) show unusual behaviour when compared with other strong emission lines in solar EUV spectra. Reviews of observations of the helium resonance lines and attempts to model their formation can be found in Hammer (1997) and Macpherson & Jordan (1999) (hereafter MJ99), but the details relevant to the present work are summarized here.

Early observations (e.g. Tousey 1967) showed that the helium resonance lines are reduced significantly in intensity in coronal holes compared with the average quiet Sun, while other lines formed at similar temperatures show only very small reductions in intensity. In the quiet Sun, the helium resonance line intensities are too large to be reproduced by emission measure distributions that account for other transition region (TR) lines, a problem identified by Jordan (1975), who found disagreements by factors of 15 for He I and 6 for He II. Corresponding factors of at least 10 and 13,

respectively, were found by MJ99. Radiative transfer calculations have also been unable to reproduce the observed resonance line intensities without invoking either a ‘plateau’ in the model atmosphere (see e.g. Vernazza, Avrett & Loeser 1981; Andretta & Jones 1997), which leads to other lines formed in the lower TR being over-estimated (Smith 2000), or some departure from equilibrium (e.g. Fontenla, Avrett & Loeser 1993; Avrett 1999). These results have been taken to imply that some process preferentially enhances the helium resonance line intensities with respect to other lines formed in the TR in the quiet Sun, and that the enhancement is reduced in coronal holes. Recent results from the Solar and Heliospheric Observatory (*SOHO*) show that the helium resonance line intensities are reduced by factors of 1.5–2.0 (Peter 1999; Jordan, Macpherson & Smith 2001) in coronal holes.

Many possible enhancement processes have been investigated, but a completely convincing explanation has not yet been found. The effects of photoionization by coronal radiation have been suggested as a natural explanation of the coronal hole/quiet Sun contrast (Zirin 1975), and

\* E-mail: g.smith2@physics.ox.ac.uk

photoionization-recombination (PR) appears to be important in the formation of some lines in the helium spectrum (He II 1640.4 Å – Wahlström & Carlsson 1994, He I 10830 Å – Andretta & Jones 1997). Although PR probably contributes to the formation of the He I 584.3-Å line, evidence (Milkey 1975; Andretta & Jones 1997; Andretta et al. 1999) suggests that the He II 303.8-Å line and, to a lesser extent, the 584.3-Å line, are formed principally by collisional excitation. If this is the case, then because the helium resonance lines have unusually large values of  $W/kT_e$ , where  $W$  is the excitation energy, their collisional contribution functions are sensitive to excitation by suprathermal electrons. Any process exposing helium ions to larger populations of suprathermal electrons than in equilibrium will tend to increase the collisional excitation rates of the helium lines, while lines with smaller  $W/kT_e$  will be relatively unaffected.

Two processes by which this might occur were suggested by Jordan (1975,1980): the transport of high energy electrons from the upper TR or corona to the lower TR, or the transport of He atoms and ions by turbulent motions to regions of higher electron temperature. Both processes would be expected to depend on the magnitude of the temperature gradient, which could explain the coronal hole/quiet Sun contrast, since Munro & Withbroe (1972) found  $dT/dh$  to be an order of magnitude smaller inside coronal holes.

Shoub (1983) investigated the former process in his study of the shape of the electron velocity distribution function (EVDF) in the transition region. His calculations suggested that EVDFs in the lower TR should have more heavily populated suprathermal tails than the local Maxwellian distribution. He found that this could lead to enhanced collisional excitation and ionization in helium, but did not calculate intensities to compare with observations. Anderson, Raymond & Ballegooijen (1996) did calculate intensities for the He II resonance line under excitation by several different non-Maxwellian EVDFs, and found enhancements over Maxwellian collisional excitation, but their calculations could not reproduce the observed intensities of all the lines they studied simultaneously.

Radiative transfer calculations of the helium resonance line intensities using EVDFs approximating those derived by Shoub (1982,1983) have been performed, and are reported in a companion paper (Smith, in preparation – hereafter paper II). The calculations suggest that the He I and He II resonance line intensities could be increased by non-Maxwellian collisional excitation, but that this process would produce signatures in the line ratios that contradict observations.

The second process is the subject of this paper. The temperature gradients in the solar TR are such that velocities of order  $10 \text{ km s}^{-1}$  could carry material into regions of significantly higher electron temperature. Such mixing could be caused by non-thermal motions in the TR that can be inferred from observations of the excess widths of optically thin lines (e.g. Berger, Bruner & Stevens 1970; Boland et al. 1973; Doschek et al. 1976; Chae, Schühle & Lemaire 1998. See also Section 2.3). Helium ions would reach statistical equilibrium at the new local temperature much more slowly than the bulk of the material owing to their long excitation and ionization times. The helium resonance lines would be excited collisionally at higher temperatures and hence with greater rates than would be the case in statistical equilibrium at the temperatures determining the ground state pop-

ulations, while other transition region lines are relatively unaffected. Jordan (1980) investigated the effects of the process on the He II 303.8-Å line, and a more extensive study has been made recently by Andretta et al. (2000), who termed the process ‘velocity redistribution.’

This work represents the application of similar methods to more specific examples of temperature gradients, which are no longer assumed to be constant over the path of the moving clump of plasma. A new treatment is used for the mean lifetime of the helium ground state, and the analysis is extended to the cases of the He I 584.3-Å and 537.0-Å lines in a first approximation.

In Section 2 earlier work on non-thermal transport of helium is reviewed, and the methods and atmospheric parameters used here to calculate the enhancements of the helium line intensities are introduced. In Section 3 the calculations of the velocity redistribution enhancement factors for the He II 303.8-Å line and the He I 584.3-Å and 537.0-Å lines are described in detail. The possible effects of non-Maxwellian electron distributions in the transition region on the calculations are assessed. In Section 4 the results of the calculations are discussed. The derived enhancement factors are compared with the results of MJ99, to determine whether the process can explain quantitatively the anomalously large helium line intensities. More qualitative comparisons are made with observations of the spatial variations of the helium line intensities in the quiet Sun with respect to each other and to other transition region lines. Comparisons are also made with the results of a separate investigation into the possibility that the helium resonance line intensities are enhanced by excitation by non-local suprathermal electrons (Paper II).

## 2 METHODS OF CALCULATION

### 2.1 Earlier work

Jordan (1980) investigated the enhancement that would occur in the He II 303.8-Å line intensity if the line were collisionally excited at a higher temperature than that appropriate to conditions of statistical equilibrium. Starting at an initial temperature of  $T_1 = 8 \times 10^4 \text{ K}$ , she assumed that He II ions are carried up the temperature gradient at the local non-thermal (macroturbulent) velocity derived from the excess widths observed in lines formed near the initial temperature. She wrote the excitation time of the ion’s ground state as the reciprocal of the collisional excitation rate (at the final temperature – see below for a discussion of this point). The excitation time and the non-thermal velocity were used to calculate a free path travelled by the ion before it is excited. The final temperature of excitation was then computed using a mean temperature gradient. Using values of the non-thermal velocity and the temperature gradient appropriate to different regions of the atmosphere (quiet Sun, coronal holes, active regions), she found intensity enhancements of up to a factor of 5. This was of the right order needed to explain the discrepancy between observed and calculated intensities reported in Jordan (1975).

Andretta et al. (2000) followed the same approach for the He II resonance line, but instead of using single upward non-thermal velocity, they considered an ensemble of

plasma elements (clumps) in an isotropic turbulent velocity field with a Gaussian distribution having a standard deviation equal to the root-mean-squared non-thermal velocity  $\sqrt{\langle v_T^2 \rangle}$ . Andretta et al. (2000) also used  $T_i = 8 \times 10^4$  K and assumed a constant pressure in the transition region. They calculated the enhancement factor over a parameter space of  $\langle v_T^2 \rangle$  and  $dT/dh$  appropriate to conditions in the TR, and for values of the electron pressure corresponding to quiet Sun and active region conditions. Enhancement factors of up to about 5 were obtained for values of the parameters typical of current models and observations of the quiet Sun transition region ( $P_e/k = 5 \times 10^{14}$  cm<sup>-3</sup> K,  $\sqrt{\langle v_T^2 \rangle} \geq 10$  km s<sup>-1</sup>,  $dT/dh \geq 10^3$  K km<sup>-1</sup>). Scaling arguments derived from their analysis show reasonable agreement with observations of the He II 303.8-Å line compared with the O III 599.6-Å line. They concluded that the process could account for at least some of the enhancement required in the 303.8-Å line intensity.

Our calculations of the effects of non-thermal motions follow the approaches of Jordan (1980) and Andretta et al. (2000), but with certain changes. The above studies used the ‘coronal approximation,’ assuming that in the resonance lines radiative decay is balanced by collisional excitation. Radiative transfer calculations suggest that this is certainly realistic in the case of the He II resonance line (Smith 2000), so this assumption is also made here. In treating the He I lines, advantage is taken of information from radiative transfer calculations made using full atmospheric models.

In the coronal approximation the enhancement factor in the intensity of the 303.8-Å line is given approximately by the ratio of the collisional excitation rate at the final temperature to that at the initial temperature. The collisional excitation rate  $C_{ij}$  is given by the expression

$$C_{ij}(T_e) = 8.63 \times 10^{-6} \frac{\Omega_{ij}}{g_i} T_e^{-1/2} N_e \exp\left(-\frac{W}{kT_e}\right) \text{ s}^{-1} \quad (1)$$

where  $g_i$  is the statistical weight of the lower level and  $\Omega_{ij}$  is the collision strength, which is approximately constant over the temperature range of interest. The intensity enhancement ratio is therefore given approximately by

$$\frac{I_f}{I_i} \simeq \frac{C_{ij}(T_f)}{C_{ij}(T_i)}. \quad (2)$$

Assuming the electron pressure to be constant in the transition region, using equation (1), this becomes

$$\frac{C_{ij}(T_f)}{C_{ij}(T_i)} = \left(\frac{T_i}{T_f}\right)^{3/2} \exp\left(\frac{W}{k} \left(\frac{1}{T_i} - \frac{1}{T_f}\right)\right). \quad (3)$$

The final temperature  $T_f$  depends on the velocity of the emitting plasma in the direction of the temperature gradient. In order to generalize the calculation of the enhancement factor to an ensemble of plasma elements Andretta et al. (2000) convolved equation (3) with a normalized Gaussian distribution of turbulent velocities with standard deviation  $\sqrt{\langle v_T^2 \rangle}$ :

$$G(v) = \frac{1}{\sqrt{2\pi\langle v_T^2 \rangle}} \exp\left(-\frac{1}{2} \frac{v^2}{\langle v_T^2 \rangle}\right) \quad (4)$$

to give an intensity ratio of

$$\frac{I_f}{I_i} = \int_{-\infty}^{\infty} \frac{C_{ij}(T_f)}{C_{ij}(T_i)} G(v) dv. \quad (5)$$

## 2.2 New formulations

Equation (5) was used in calculations of the enhancement factors in the present work, but the free path and final temperature  $T_f$  of each plasma element were computed by different methods to those used by Jordan (1980) and Andretta et al. (2000). These new techniques use the temperature gradient (now allowed to change over the path of the clump of plasma) derived from emission measure distributions found from observations of other transition region lines. Specific values of  $\langle v_T^2 \rangle(T_i)$  suggested by observations were used. For the 584.3-Å and 537.0-Å lines of He I the excitation rate ratio in equation (3) was also modified.

Both Jordan (1980) and Andretta et al. (2000) defined the lifetime of the ground state as  $\tau = (C_{ij}(T_f))^{-1}$ . This provides a lower limit on the lifetime and hence on the final temperature reached by the moving plasma. This may be appropriate if ions are carried rapidly to a higher temperature and remain there until excited. Here we use  $\tau = (C_{ij}(T_i))^{-1}$ , as we consider this timescale to better reflect the dependence of the enhancement process in question on the long excitation and ionization times of the helium ions at the equilibrium temperatures of resonance line formation. It is these timescales, long with respect to those for other TR lines, which allow unresolved turbulent motions to carry helium ions to the higher temperatures where excitation occurs.

$T_i$  is chosen to represent the ‘normal’ temperature of resonance line formation, in the absence of non-equilibrium processes.  $T_f$  is found by integrating the temperature gradient over the path traversed in time  $\tau$ . The (varying) temperature gradient between  $T_i$  and  $T_f$  is derived from the mean intrinsic emission distribution (EMD; see Section 2.3). The intrinsic emission measure is defined as

$$Em(0.3) = \int_{\Delta h'} N_e N_H dh \quad (6)$$

where  $N_e$  and  $N_H$  are electron and hydrogen number densities respectively and  $\Delta h'$  is defined as the interval of height in a plane-parallel atmosphere corresponding to  $\Delta(\log T_e) = 0.3$  dex, the temperature interval over which most lines are typically formed. Defining electron and hydrogen pressures as  $P_e = N_e T_e$  and  $P_H = N_H T_e$ , the emission measure may be re-written as an integral over the temperature interval in which a line is formed:

$$Em(0.3) = \int_{T_e'/\sqrt{2}}^{\sqrt{2}T_e'} \frac{P_e P_H}{T_e^2} \frac{dh}{dT_e} dT_e. \quad (7)$$

$T_e'$  is the temperature at which the line contribution function peaks, and is the geometric mean of the limits of the integral, which represent a change in  $T_e$  of a factor of 2. If  $P_e$ ,  $P_H$ , and  $dh/dT_e$  are each averaged over the temperature range of the integral, the emission measure becomes

$$Em(0.3) = \frac{P_e P_H}{\sqrt{2} T_e} \overline{\frac{dh}{dT_e}}. \quad (8)$$

The assumption of constant pressures over the region of line formation is a good one, and although the assumption of a constant temperature gradient in the same region is less good, it is often used in constructing an initial model from the EMD (see e.g. Jordan & Brown 1981).

If the mean EMD as a function of temperature is known from several lines, the path of material travelling up the tem-

perature gradient can be divided into smaller temperature intervals. Here we use intervals of 0.1 dex in  $\log T_e$ . In each of these intervals, the mean temperature gradient is calculated from the EMD, at the mean value of  $\log T_e$ , using equation (8). In most of the temperature range of interest, hydrogen is fully ionized and  $N_H = 0.83N_e$ . This is a very good approximation above  $\log T_e = 4.9$  (i.e. in the He II calculation), and is correct to better than 10 per cent down to  $\log T_e = 4.5$  (the temperature range of the He I calculation). Thus, in plane-parallel geometry, taking  $P_H = 0.83P_e$ , the increment of height  $\Delta h$  corresponding to the temperature interval  $\Delta(\log T_e)$  is given approximately by

$$\Delta h = Em(0.3) \frac{\sqrt{2T_e}}{0.83P_e^2} \Delta T_e \quad (9)$$

where  $\Delta T_e$  spans the range  $\log T_e \pm 0.05$ . The travel time required by a clump of material to traverse each  $\Delta h$  is determined by assuming a constant upward velocity  $v$ . The definition of  $\Delta h$  thus introduces a quantization of the (logarithmic) temperatures used in calculating the enhancement factor. For computational convenience this is carried over into the integration over velocities in equation (5). In this formulation, the integrand may only be evaluated correctly for values of  $T_f$  occurring at intervals of 0.1 dex in  $\log T_e$  from the initial temperature  $T_i$  ( $\log T_f = \log T_i + 0.1n$ , for integer  $n$ ). The values of  $v$  used as points in the integration correspond to velocities required to reach these  $T_f$  in a time equal to the lifetime of the ion's ground state at  $T_i$ . The velocity mesh that results introduces some uncertainty into the calculation of the enhancement factors.

### 2.3 Atmospheric parameters

The EMDs used here to derive the variation of temperature with height in the lower TR were determined from observed line fluxes and the appropriate atomic data using now-standard methods (see MJ99 and references therein). MJ99 derived separate EMDs for mean network and cell interior regions from observations of UV lines from the quiet Sun transition region made using the CDS (Coronal Diagnostic Spectrometer) and SUMER (Solar Ultraviolet Measurements of Emitted Radiation) instruments on board *SOHO*. Equation (8), used to determine the temperature gradient from the emission measure, assumes a one-component plane-parallel atmosphere. In the network model proposed by Gabriel (1976), open magnetic field lines are most vertical over the boundaries, but expand into the corona with a horizontal component in the cell interiors. Since we adopt a plane parallel atmosphere we use the network boundary EMD of MJ99 as the observed EMD.

Of the lines observed by MJ99, those formed at temperatures below  $10^5$  K (except for He II) were observed with SUMER, and those formed at higher temperatures (and the helium lines) were observed with CDS. MJ99 found that the relative intensities of the He I lines observed with CDS and with SUMER in second order suggest that the SUMER lines might need to be reduced in intensity by a factor of 1.5 if the Landi et al. (1997) CDS calibration were adopted. This would lead to the emission measure distribution below  $10^5$  K, derived from the SUMER lines, being lowered relative to the higher temperature part derived from the CDS lines.

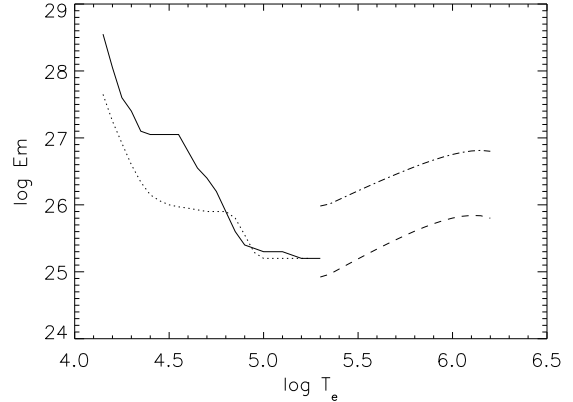


**Figure 1.** Network emission measure distributions. For  $\log T_e \leq 5.3$ , the solid line shows EMD S, the dotted line shows EMD X. Theoretical EMDs are shown for  $\log T_e > 5.3$ , with (a)  $P_e(\log T_e = 5.3) = 2 \times 10^{14} \text{ cm}^{-3} \text{ K}$  (dashed), and with (b)  $P_e(\log T_e = 5.3) = 6 \times 10^{14} \text{ cm}^{-3} \text{ K}$  (dot-dashed).

This uncertainty inspired the use of a second EMD, derived from observations of  $\xi$  Boo A, a G8 V star, made with the Goddard High Resolution Spectrograph (GHRS) instrument on the Hubble Space Telescope (Smith 2000). The EMD was scaled by a constant factor such that its minimum (at  $1 - 2 \times 10^5$  K) fits the minimum of the network emission measure of MJ99. The resulting EMD is lower, by up to an order of magnitude, at temperatures below  $\log T_e = 4.8$ , but is very similar to the solar EMD at higher temperatures. Jordan et al. (1987) found that below  $T_e \sim 10^5$  K the emission measure distributions of main sequence stars with hot coronae have approximately the same dependence on  $T_e$ , which is supported by a direct linear correlation between the C II and C IV emission line fluxes in such stars (Rutten et al. 1991). Capelli et al. (1989) found that the C II - C IV correlation also holds for solar observations at various spatial resolutions.

The discrepancy between the *SOHO* observations and the earlier results may be due in part to the different spatial resolutions of the two instruments used (CDS and SUMER). A more serious problem is that SUMER could not observe the same location on the Sun in all of the lower TR lines, or the same location at the same time as in the CDS observations (see Jordan et al. 2001). Thus there are fundamental uncertainties in the shape of the EMD derived from *SOHO* observations at temperatures below  $\log T_e \simeq 4.9$ . The  $\xi$  Boo A EMD was therefore used to explore the possible effects of this uncertainty on the present calculations. The solar EMD derived by MJ99 is hereafter referred to as EMD S, and that based on the  $\xi$  Boo A EMD is referred to as EMD X; they are shown in Figure 1.

The lines observed by MJ99 did not allow determination of the full EMD above  $\log T_e = 5.3$ . The EMDs used in the present calculations above this temperature are therefore based on energy balance arguments described below (see also Jordan 2000 and Philippides 1996).

In the lower TR, below  $\log T_e \simeq 5.0$ , some non-thermal source of heating is required to account for the rising emission measure at low temperatures. In the upper TR, however, the radiation losses are small compared with the con-

ductive flux from the corona, and may be balanced by energy deposited by the divergence of the conductive flux, or, if that flux is conserved, by a small amount of additional heating. The EMDs used here were determined assuming the former to be the case above  $\log T_e = 5.3$ . The equation expressing energy balance as a function of height in this region is then

$$\epsilon_R = -\frac{1}{A(r)} \frac{d(A(r)F_C)}{dr} \quad (10)$$

where  $\epsilon_R$  is the rate of radiative energy loss per unit volume, and  $F_C$  is the classical conductive energy flux through an area  $A(r)$  normal to the radial co-ordinate  $r$ . The radiation loss term is given by

$$\epsilon_R = N_e N_H P_{\text{rad}}(T_e) \quad (11)$$

where  $P_{\text{rad}}(T_e)$  is the radiative power loss in all lines and continua, as a function of temperature in a plasma of known composition.  $P_{\text{rad}}(T_e)$  is calculated here using the power law fit to the radiative power loss curve adopted by Philippides (1996):

$$P_{\text{rad}}(T_e) = 1.25 \times 10^{-16} T_e^{-1} \text{ erg cm}^3 \text{ s}^{-1}. \quad (12)$$

$F_C$  is given by

$$F_C(T_e) = -\kappa T_e^{5/2} \frac{dT_e}{dr} \quad (13)$$

where the Spitzer-Härm conductivity  $\kappa \simeq 1.1 \times 10^{-6} \text{ erg cm}^{-1} \text{ K}^{-7/2} \text{ s}^{-1}$  at  $T_e = 10^6 \text{ K}$  (Spitzer 1956). That value is used here, as  $\kappa$  is only 30% smaller at  $T_e = 10^5 \text{ K}$ . Energy transfer by mass motions of any kind (including the turbulent motion assumed in the enhancement factor calculations) is not considered in the energy balance equation used in the upper TR.

Combining the energy balance equation (10) with equation (8) for the emission measure in terms of the temperature gradient gives an expression for the logarithmic gradient of the emission measure with temperature (Jordan 2000):

$$\frac{d \log Em(0.3)}{d \log T_e} = \frac{3}{2} + 2 \frac{d \log P_e}{d \log T_e} + \frac{d \log A(T_e)}{d \log T_e} - \frac{2Em(0.3)^2 P_{\text{rad}}(T_e)}{0.83\kappa P_e^2 T_e^{3/2}}. \quad (14)$$

Assuming forms for  $P_e(T_e)$  and  $A(T_e)$ , this equation may be integrated numerically from given boundary conditions to give the emission measure as a function of temperature in that part of the atmosphere where the energy balance is described by equation (10). In this case the electron pressure was assumed to vary according to hydrostatic equilibrium (the use of a constant value of  $P_e$  in equation (3) in calculating the intensity enhancement is a good approximation in the lower TR, owing to its small vertical extent).  $A(T_e)$  was taken only to vary with the expansion with height of a spherically symmetric atmosphere; assuming that emission comes from a uniform layer at each height, this is consistent with the use of the empirical EMDs derived in the plane-parallel approximation in the lower TR, because the small extent of that part of the atmosphere makes the two approaches approximately equivalent.

The assumptions about  $A(T_e)$  represent a significant simplification. The EMD derived below  $\log T_e = 5.3$  represents an average over any unresolved structure within the network boundaries, while the EMD computed using

equation (14) is the ‘intrinsic’ value; they are unlikely to match at  $\log T_e = 5.3$ . If the calculated emission measure at  $\log T_e = 5.3$  is greater than the value derived from spatially averaged observations, this implies that only some fraction of the observed region is occupied by emitting material.

With the assumed forms for  $P_e(T_e)$  and  $A(T_e)$ , the EMD for the upper TR was determined using equation (14), choosing values of the emission measure, electron pressure, and coronal temperature  $T_C$  at the top of the region.  $T_C$  was chosen such that  $\log T_C = 6.20$ , as CDS observations suggest that there is little material at higher temperatures in the quiet corona (Landini & Landi 1998). For a given coronal pressure and temperature, the coronal emission measure cannot exceed a certain value if the RHS of equation (14) is to remain positive above  $\log T_e = 5.3$ , as is required by the observed gradient of the EMD. There is hence a ‘critical solution,’ with the largest possible value of the coronal emission measure which reproduces the observed minimum in the EMD at  $\log T_e \simeq 5.3$ . If  $Em(T_C)$  is larger than this value, conduction from the corona deposits more energy in the upper TR than can be lost by radiation.

The mean pressure in the boundary regions used in deriving EMD S below  $\log T_e = 5.3$  was found by MJ99 to be  $\log P_e = 14.27$ , with a standard deviation of  $\pm 0.35$ . Using a coronal pressure that reproduces this pressure ( $\simeq 2 \times 10^{14} \text{ cm}^{-3} \text{ K}$ ) at  $\log T_e = 5.3$  in the critical solution gives EMD (a) shown in Figure 1. This is lower than the observed emission measure at  $\log T_e = 5.3$ , suggesting that a slightly higher pressure is needed for a continuous EMD through this temperature. EMD (a) also predicts substantially less Mg IX and Mg X emission than observed by MJ99 (when the photospheric abundance of Mg is used in both  $P_{\text{rad}}(T_e)$  and in calculating the line intensities). There are problems with such a comparison, however, as the intensities used by MJ99 correspond to areas defined as network boundaries in the CDS transition region lines, and the details of the connection between the TR network and the corona are unknown. Open field regions would be expected to expand in the corona, but the network boundaries may also contain closed field emitting regions unconnected to the corona.

Figure 1 also shows EMD (b), a second upper TR EMD calculated to give a higher transition region pressure of  $P_e = 6 \times 10^{14} \text{ cm}^{-3} \text{ K}$ , which corresponds to the largest pressures found by MJ99 (in cell interiors) and is similar to values used in earlier models of the atmosphere (e.g. Vernazza et al. 1981). It provides a much better match to the Mg IX and Mg X data, although, as stated above, these do not provide a stringent constraint. EMD (b) predicts an intrinsic emission measure at  $\log T_e = 5.3$  that is larger than the apparent (plane-parallel) emission measure. This discontinuity can be explained in terms of an area filling factor below  $\log T_e = 5.3$  (see Sim & Jordan 2001). For a filling factor  $A_i/A_{\text{obs}}$ , the intrinsic emission measure below  $\log T_e = 5.3$  is

$$Em_i = \frac{A_{\text{obs}}}{A_i} Em_{\text{app}} \quad (15)$$

where  $Em_{\text{app}}$  is shown in Figure 1. In the theoretically derived upper TR the filling factor is assumed to be 1.0. Scaling the lower TR EMD to match the upper TR EMD (b) at  $\log T_e = 5.3$  suggests a filling factor in the lower TR of 0.16 (within the area of  $\sim 3.4 \text{ arcsec}^2$  resolved by CDS). The continuous EMD then describes the restricted areas where the

filling factor is 1.0. The lines used to find the lower TR EMD are not sensitive to  $P_e$ , so a similar matching procedure may be considered for any lower pressure above about  $2.7 \times 10^{14} \text{ cm}^{-3} \text{ K}$ , for which the theoretical upper EMD would match the observed emission measure at  $\log T_e = 5.3$ , with a filling factor of 1.0. Equations (8) and (15) show that the temperature gradient derived from  $Em(T_e)$  scales as  $P_e^2 A_i/A_{\text{obs}}$ , but the value of  $A_i/A_{\text{obs}}$  (i.e. the factor by which the theoretical and observed EMDs differ at  $\log T_e = 5.3$ ) required for a continuous EMD through  $\log T_e = 5.3$  scales as  $P_e^{-2}$ . If the filling factor in the lower TR is regarded as a free parameter, the distribution of  $dT_e/dh$  is the same for all continuous EMDs in which a lower TR EMD is scaled to match an upper TR EMD, and it is independent of the assumed pressure.

The distributions of  $dT_e/dh$  derived in this manner for the cases of lower TR EMDs S and X were used in the calculations of the helium line enhancement factors. In order to investigate the effect of the possible solutions suggested by EMDs (a) and (b), the calculations were performed for electron pressures representing these limits,  $P_e = 2 \times 10^{14} \text{ cm}^{-3} \text{ K}$  and  $P_e = 6 \times 10^{14} \text{ cm}^{-3} \text{ K}$  (the lower pressure is not technically consistent with the filling factor argument, but, considering other approximations involved in the calculations, provides a useful lower limit). Because the temperature gradients used in the enhancement factor calculations are independent of the assumed pressure, the pressure adopted influences only the excitation time. The excitation time scales as  $P_e^{-1}$ ; hence the velocity required to reach a given  $T_f$ ,  $v(T_f)$ , scales as  $P_e$ . A higher pressure will therefore lead to larger  $v(T_f)$ , causing contributions from higher temperature regions to be suppressed by the Gaussian term,  $G(v)$ , in the enhancement factor integral.

The values of  $\langle v_T^2 \rangle$  used in the integral in equation (5) were determined from empirical relations fitted to observational data. From early rocket experiments (e.g. Berger et al. 1970; Boland et al. 1973) to recent results from *SOHO* (e.g. Chae et al. 1998; Peter 2001), solar observations of optically thin TR lines have shown widths in excess of those due to thermal motion at the temperatures at which the lines are thought to form. The non-thermal component of the broadening could be due to unresolved upflows and downflows, to acoustic or MHD waves, or to small scale turbulence. We interpret the non-thermal widths in the TR as evidence of turbulent motions of unspecified origin. Since the line profiles are approximately Gaussian, assuming a Gaussian distribution of non-thermal velocities allows the most probable turbulent velocity  $\xi$  to be extracted from the line width using the expression

$$\frac{\Delta\lambda}{\lambda} = \frac{2\sqrt{\ln 2}}{c} \left( \frac{2kT_{\text{ion}}}{m_{\text{ion}}} + \xi^2 \right)^{1/2} \quad (16)$$

where  $\Delta\lambda$  is the full width at half maximum,  $\lambda$  is the wavelength of the line,  $T_{\text{ion}}$  is the ion temperature of line formation, and  $m_{\text{ion}}$  the mass of the emitting ion. The mean squared non-thermal velocity  $\langle v_T^2 \rangle$  is given by the relation  $\langle v_T^2 \rangle = (3/2)\xi^2$ .

Up to  $\log T_e \sim 5.3$ , both recent *SOHO* measurements of  $\xi^2$  (Chae et al. 1998) and earlier measurements (see Jordan 1991) are fitted quite well by the relation  $\xi^2 \propto T_e^{1/2}$ , which would be expected if a wave flux from lower regions were

conserved through the transition region to be dissipated at greater heights. The values of  $\langle v_T^2 \rangle(T_i)$  used in the present study are found using

$$\xi = 25 \left( \frac{T_e}{2 \times 10^5 \text{ K}} \right)^{1/4} \text{ km s}^{-1}. \quad (17)$$

The value of  $\xi^2$  and hence  $\langle v_T^2 \rangle$  used to characterize the velocity field in each calculation was taken to be the value given by equation (17) at the initial temperature  $T_i$ .

Peter (2001) has found that some transition region lines (forming in the temperature range  $4.6 \leq \log T_e \leq 5.8$ ) can be fitted more precisely with two Gaussian components. The widths of the core components are similar to those found by Chae et al. (1998); the widths of the broad components are significantly larger, but are also consistent with  $\xi^2 \propto T_e^{1/2}$ . Peter (2001) interprets the broad components as evidence of the passage of magnetoacoustic waves in coronal funnels in the network. It is not known whether the (optically thick) helium lines have this broad component. If larger turbulent velocities were assumed in the present calculations, contributions from higher temperatures would become more important and the enhancement factors derived would be larger. The temperature dependence of  $\xi^2$  would mean that the enhancement factors for He II would be increased by a relatively greater amount than those for He I.

### 3 ENHANCEMENT FACTOR CALCULATIONS

#### 3.1 The He II 303.8-Å line

Radiative transfer calculations with a 39 level model helium atom (Smith 2000) show that the contribution function to the intensity of the 303.8-Å line peaks at  $\log T_e \simeq 4.9$ , and this value was used for  $\log T_i$  in the integration of equation (5) for the He II line. The same peak formation temperature was found by MJ99 using the ionization equilibrium of Arnaud & Rothenflug (1985) assuming purely collisional excitation, which is consistent with the model calculations. At  $\log T_i = 4.9$ ,  $\sqrt{\langle v_T^2 \rangle(T_i)} = 24.3 \text{ km s}^{-1}$ . The collisional excitation rate  $C_{ij}(T_e)$  for the He II resonance transition was calculated using equation (1), taking  $P_e$  as constant and using the collision strength  $\Omega_{ij}(T_e)$  given by Aggarwal et al. (1992). This rate was also used to calculate the lifetime of the ground state,  $\tau = C_{ij}^{-1}$ . The He II excitation time at this temperature is 5.69 s, compared with a time of 0.06 s for the O III 599.6-Å line, using the collision strengths of Aggarwal (1993), and  $3 \times 10^{-3} \text{ s}$  for the C IV 1548-Å lines (Mariska 1992), formed at slightly higher temperatures of  $\log T_e \simeq 5.0$  (these times assume  $P_e = 6 \times 10^{14} \text{ cm}^{-3} \text{ K}$ ). The differences imply that other lines formed at similar temperatures to the He II 303.8-Å line would be relatively unaffected by turbulent transport.

In order to facilitate a discussion of some of the interesting features and limitations of the enhancement factor calculations, details of the calculations are presented in Table 1 and Figures 2 and 3. Table 1 shows the heights above  $T_i$  corresponding to the final temperatures  $T_f$  determined from the EMDs using equation (9). Figure 2 shows the excitation rate ratio as a function of  $\log T_e$ , and Figure 3 illustrates the form of the integrand in equation (5), showing the contribution to the total intensity enhancement of plasma elements

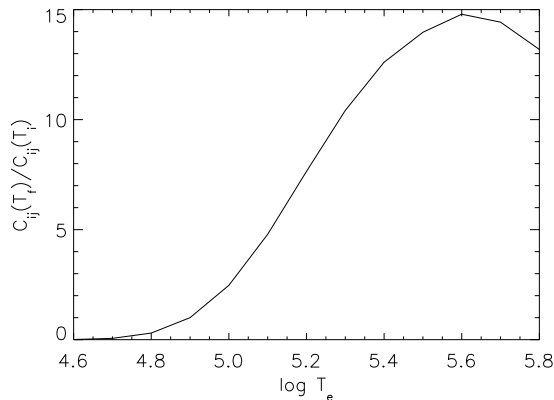


**Figure 2.** The excitation rate ratio  $C_{ij}(T_f)/C_{ij}(T_i)$  as a function of (logarithmic) temperature for the He II 303.8-Å line, as used in calculations of the enhancement factors.  $\log T_i = 4.9$ .

**Table 1.** Final temperatures and heights above  $\log T_i = 4.9$  reached by plasma elements with velocity  $v(T_f)$ , computed using EMDs S and X. An assumed pressure of  $P_e = 2 \times 10^{14} \text{ cm}^{-3}$  K is denoted by (a),  $P_e = 6 \times 10^{14} \text{ cm}^{-3}$  K is denoted by (b). Values of  $T_f < T_i$  correspond to downward-moving elements.

$\log T_f$	$h(T_f) - h(T_i)$ (km)		$v(T_f)$ (km s <sup>-1</sup> )			
	S	X	S(a)	X(a)	S(b)	X(b)
4.6	-84.4	-44.8	-4.94	-2.62	-14.8	-7.87
4.7	-38.2	-33.7	-2.24	-1.97	-6.71	-5.92
4.8	-13.0	-17.3	-0.762	-1.01	-2.28	-3.04
5.0	11.6	12.3	0.680	0.721	2.04	2.16
5.1	28.0	25.3	1.64	1.48	4.92	4.45
5.2	51.2	45.9	3.00	2.69	9.00	8.07
5.3	83.9	78.6	4.92	4.60	14.7	13.8
5.4	140	135	8.20	7.91	24.6	23.7
5.5	262	257	15.3	15.1	46.0	45.2
5.6	518	513	30.3	30.1	91.0	90.2
5.7	1070	1060	62.4	62.1	187	186
5.8	2190	2180	128	128	384	383

with different velocities. The velocities required to reach  $T_f$  are listed in Table 1. The quantization of  $\log T_e$  and  $h$  produces a fine mesh of velocities at and below the peak in the excitation rate ratio, but a coarser grid at higher temperatures. This results in some over-estimation of the total He II enhancement factor, particularly in the contribution from the material with  $v > 30 \text{ km s}^{-1}$ . Rough calculations suggest this over-estimation could be by about 10–20 per cent.

The calculations made assuming  $P_e = 6 \times 10^{14} \text{ cm}^{-3}$  K show the peak contribution to the intensity occurring for upward velocities of about  $15 \text{ km s}^{-1}$ , but with a significant contribution from faster-moving material. The contribution of material moving downwards ( $v < 0$ ) is seen to be negligible. The peak contribution to the intensity occurs at  $\log T_e = 5.3$ , at a height above  $T_i$  of about 80 km. EMDs S and X lead to similar temperature profiles, resulting in similar enhancement factors being derived for each, 5.3 for EMD S and 5.5 for EMD X.

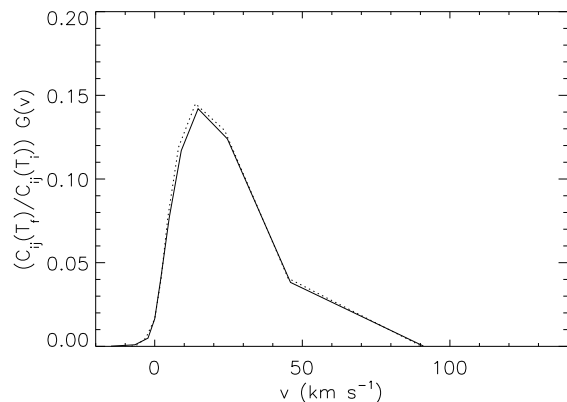
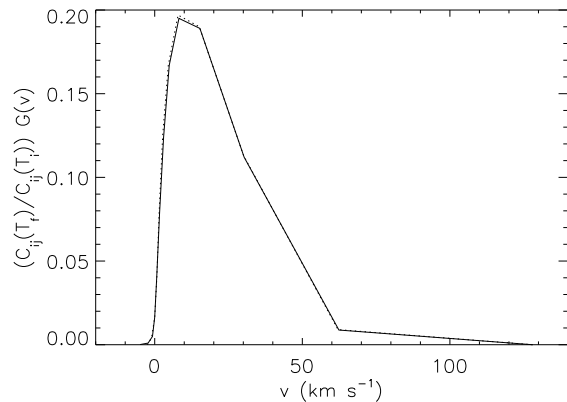


**Figure 3.** The integrand in equation (5) for the intensity enhancement, evaluated for the He II resonance line, using EMD S (solid) and EMD X (dotted) with  $P_e = 2 \times 10^{14} \text{ cm}^{-3}$  K (top) and  $P_e = 6 \times 10^{14} \text{ cm}^{-3}$  K (bottom).

Assuming a lower pressure with these EMDs produces larger enhancement factors, as predicted in Section 2.3. The total enhancement factors computed for  $P_e = 2 \times 10^{14} \text{ cm}^{-3}$  K are 6.9 for EMD S and 7.0 for EMD X. Figure 3 and Table 1 show that the peak contribution to the intensity occurs at a greater height and temperature than at the higher pressure, as the velocities required to reach given  $T_f$  are decreased (because the excitation time is longer).

### 3.2 The He I 584.3-Å and 537.0-Å lines

Similar calculations were performed for the first two lines of the He I resonance series, although here the situation is more complicated, as the coronal approximation no longer applies. First, the He I resonance lines form at greater optical depths than the He II line, and full radiative transfer modelling is required to compute their intensities properly. Even neglecting transfer of photons within the line, direct collisional excitation is in general not the dominant excitation process in radiative transfer calculations (Hearn 1969; Andretta & Jones 1997; Smith 2000). Those calculations reveal that important contributions come from radiative transitions from levels other than the ground state, which are themselves populated by a combination of collisional excitation and radiative recombination. Neither the excitation rate

nor the mean lifetime of the He I ground state can be accurately evaluated using the equivalent expression to equation (1) used in the He II calculation. In order to investigate the possible effect of non-thermal motions on the 584.3-Å ( $1s2p\ ^1P - 1s^2\ ^1S$ ) and 537.0-Å ( $1s3p\ ^1P - 1s^2\ ^1S$ ) lines in a first approximation, corrections were made to the expressions used to compute these quantities. Radiative transfer effects were not considered.

Radiative transfer calculations (Smith 2000) reveal that significant contributions to the  $2\ ^1P$  level population come from allowed radiative transitions from other singlet levels, especially  $2\ ^1S$ ,  $3\ ^1S$ , and  $3\ ^1D$ . These levels are collisionally excited from the ground at high temperatures but largely populated by radiative recombination at low temperatures. The collisional contribution to the population of the  $2\ ^1P$  level through these channels was approximated in the calculation of the velocity redistribution enhancement factor by writing the total excitation rate  $C'_{ij}(T_e)$  as

$$C'_{ij}(T_e) = C_{ij}(T_e) + \sum_{k \neq j} \left( \frac{A_{kj}}{\sum_l A_{kl}} C_{ik}(T_e) \right) \quad (18)$$

where  $C_{ij}(T_e)$  is the direct collisional excitation rate, and the second term is the sum of the collisional excitation rates of the other contributing levels, multiplied by radiative branching ratios.  $C_{ij}(T_e)$  and  $C_{ik}(T_e)$  were evaluated using expression (1), with collision strengths for  $T_e = 3 \times 10^4$  K (the collision strengths were assumed to be constant at higher temperatures, as their variation at higher  $T_e$  was often unavailable) provided by Lanzafame et al. (1993) and Sawey & Berrington (1993). The Einstein  $A$ -values were taken from Drake (1996).

The excitation rate ratio was calculated using  $\log T_1 = 4.5$ . This temperature was found by MJ99 to represent the peak of formation of the 584.3-Å line. Radiative transfer calculations (Smith 2000) suggest a slightly lower temperature  $\log T_1 \simeq 4.45$  due to a different ionization balance, but as comparisons are being made here with MJ99, the former figure was kept. Using a lower  $T_1$  would have relatively little effect on the final temperatures responsible for the velocity redistribution intensity enhancement, as at  $\log T_1 \simeq 4.45$ , excitation times for the He I resonance line are so long (about 40 s; Smith 2000) that ions in the ground state are very likely to survive at least to  $\log T_1 = 4.5$ , and their subsequent behaviour to be determined by higher temperatures (as for He II, peak enhancement occurs where  $\log T_e > 5.0$ ). The absolute value of the intensity enhancement is, however, more significantly affected by the choice of  $T_i$ , through the excitation rate ratio. The total collisional excitation rate calculated using equation (18) is a factor of two smaller at  $\log T_1 = 4.45$  than at  $\log T_1 = 4.5$ , so choosing a lower  $T_1$  would be expected to produce a larger enhancement.

The expression used for the excitation rate is a less exact approximation to the true rate than in the case of He II, neglecting as it does the effects of recombination, which is probably important in the formation of the He I resonance lines (Andretta & Jones 1997; Smith 2000). Recombination is most significant below the peak temperature of line formation. At  $\log T_e \geq 4.5$ , the temperature range considered here, the expression used represents about 75 per cent of the total excitation rate computed in radiative transfer calculations. The fraction does not change significantly with

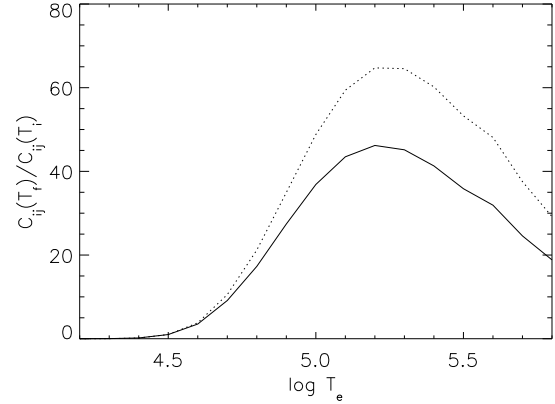


**Figure 4.** The excitation rate ratio  $C'_{ij}(T_f)/C'_{ij}(T_1)$  as a function of (logarithmic) temperature for the He I 584.3-Å (solid) and 537.0-Å (dotted) lines, as used in calculations of the enhancement factors.  $\log T_1 = 4.5$ .

temperature in this range. As the enhancement factor due to non-thermal transport of He depends on relative rates at  $T_f$  and  $T_1$ , this approximation should have little effect on the effect on the calculated values of the enhancement factors.

Whereas in He II the collisional excitation of the resonance line completely dominates the depopulation of the ground state, in He I there are competing processes which act to shorten the lifetime of the ground state, some of which do not result in excitation to the  $2\ ^1P$  level. Collisional excitation rates to other bound levels are significant, as considered above, and collisional ionization becomes important at high temperatures. Hence the probability that a given He I ion survives in the ground state until reaching  $T_f$  is smaller than would be determined by simply taking the reciprocal of  $C'_{ij}$  (equation (18)). In order to take this shortening of the *effective* excitation time into account in a first approximation, for He I  $\tau(T_i)$  was calculated by removing the radiative branching ratios from the expression for  $C'_{ij}$  and adding the collisional ionization rate (Mihalas & Stone 1968) before taking the reciprocal to give a mean lifetime (no longer strictly an ‘excitation time’).

Using these new prescriptions for determining  $C'_{ij}(T_i)$  and  $\tau(T_i)$ , the intensity enhancement integrals for the 584.3-Å line were performed as for the He II resonance line, with  $\sqrt{\langle v_T^2 \rangle}(T_1) = 19.4\ \text{km s}^{-1}$  and  $\tau(T_1) = 10.5\ \text{s}$  (this time may be compared with the excitation times, at the same temperature, of the C II lines near 1335 Å of about 0.05 s – Smith 2000). Details of the integrals are presented in Figures 4 and 5 and Table 2. These show that assuming  $P_e = 6 \times 10^{14}\ \text{cm}^{-3}\ \text{K}$  with EMD S predicts the peak contribution to the intensity to come from material with  $v \simeq 20\ \text{km s}^{-1}$ , reaching  $\log T_e \simeq 5.1$  at a height of about 200 km above  $T_1$ . Significant contributions are again seen from material reaching higher temperatures. Taking  $P_e = 2 \times 10^{14}\ \text{cm}^{-3}\ \text{K}$  with EMD S, the peak contribution comes from slower-moving material ( $v < 10\ \text{km s}^{-1}$ ), but because the excitation time is longer at the lower pressure, this material reaches greater heights and is excited at higher temperatures. The total enhancement factor is correspondingly increased: 15.3



**Table 2.** Final temperatures and heights above  $\log T_i = 4.5$  reached by plasma elements with velocity  $v(T_f)$ , computed using EMDs S and X. An assumed pressure of  $P_e = 2 \times 10^{14} \text{ cm}^{-3}$  K is denoted by (a),  $P_e = 6 \times 10^{14} \text{ cm}^{-3}$  K is denoted by (b). Values of  $T_f < T_i$  correspond to downward-moving elements.

$\log T_f$	$h(T_f) - h(T_i)$ (km)		$v(T_f)$ (km s $^{-1}$ )			
	S	X	S(a)	X(a)	S(b)	X(b)
4.2	-181.5	-30.3	-5.77	-0.963	-17.3	-2.89
4.3	-99.3	-13.1	-3.16	-0.416	-9.47	-1.25
4.4	-58.1	-5.95	-1.85	-0.189	-5.54	-0.567
4.6	92.4	7.68	2.94	0.244	8.81	0.732
4.7	139	18.8	4.42	0.597	13.3	1.79
4.8	164	35.2	5.21	1.12	15.6	3.36
4.9	177	52.5	5.62	1.67	16.9	5.00
5.0	188	64.8	5.97	2.06	17.9	6.18
5.1	205	77.8	6.51	2.47	19.5	7.42
5.2	228	98.4	7.24	3.13	21.7	9.38
5.3	261	131	8.29	4.16	24.9	12.5
5.4	317	187	10.1	5.94	30.2	17.8
5.5	439	309	13.9	9.82	41.8	29.5
5.6	695	565	22.1	18.0	66.3	53.9
5.7	1240	1110	39.5	35.3	118	106
5.8	2360	2230	75.1	70.9	225	213

for  $P_e = 2 \times 10^{14} \text{ cm}^{-3}$  K compared with 11.2 for  $P_e = 6 \times 10^{14} \text{ cm}^{-3}$  K. This can be seen clearly in Figure 5.

For both values assumed for the pressure, the total enhancement factors computed using EMD X are larger than for EMD S. A factor of 17.6 is found for  $P_e = 2 \times 10^{14} \text{ cm}^{-3}$  K and a factor of 18.7 is found for  $P_e = 6 \times 10^{14} \text{ cm}^{-3}$  K. In both cases the peak in the intensity contribution occurs at  $\log T_e = 5.2$  at a height of about 100 km above  $T_i$ . The velocities required to reach this  $T_f$  are smaller than in the calculations using EMD S, as the temperature gradients derived from EMD X in the lower TR are larger. The Gaussian weighting leads to the larger enhancements found with EMD X. The factors computed for He II using the two EMDs are more similar because the (lower TR) EMDs themselves are similar above the initial temperature ( $\log T_i = 4.9$ ).

Although the use of  $\log T_i = 4.5$  for the He I resonance line may lead to under-estimation of the enhancement factors if the line forms in equilibrium at a slightly lower temperature, other approximations used in the calculations tend to lead to over-estimation. In comparing with the work of MJ99, who assumed line formation at  $\log T_e = 4.5$ , the figures derived here should therefore be regarded as upper limits on the possible enhancement factors. This can be seen in the fact that the enhancement of the 584.3-Å line is found to increase with pressure in calculations using EMD X, showing that the uncertainties introduced by the large velocity steps in the tail of the integrand are significant in this case.

MJ99 did not compare the observed intensity of the He I 537.0-Å line directly with the EMD derived from ‘normal’ transition region lines, but radiative transfer calculations under-produce the observed intensity of this line by factors of the same order as in the 584.3-Å line (Smith 2000). Enhancement factors were therefore computed for the 537.0-Å line, focusing on a comparison with the 584.3-Å line. Indirect collisional excitation (mainly through the  $2^1S$ ,  $4^1S$

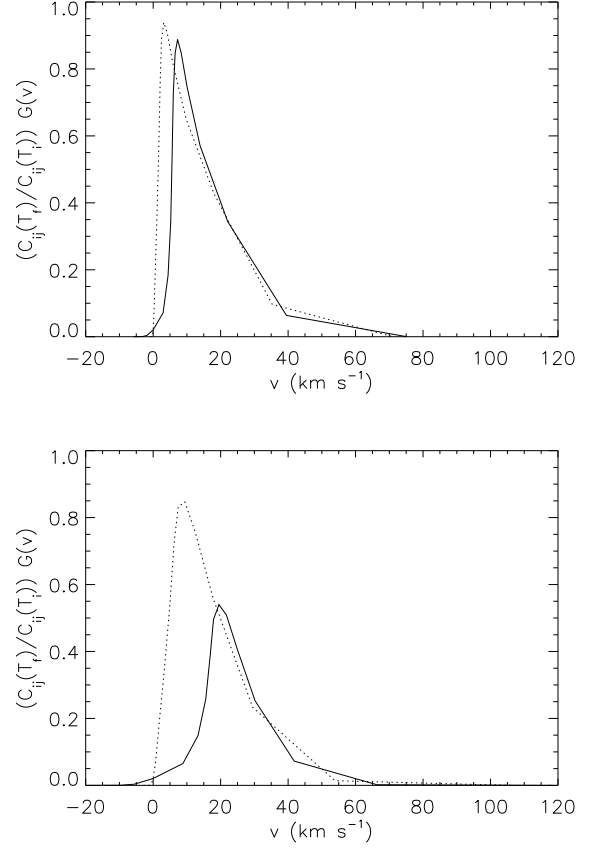


**Figure 5.** The integrand in equation (5) for the intensity enhancement, evaluated for the He I resonance line, using EMD S (solid) and EMD X (dotted) with  $P_e = 2 \times 10^{14} \text{ cm}^{-3}$  K (top) and  $P_e = 6 \times 10^{14} \text{ cm}^{-3}$  K (bottom).

and  $4^1D$  levels) was again included in the total excitation rates calculated for  $T_i$  (again  $\log T_i = 4.5$ ) and  $T_f$  and in the calculation of the mean ground state lifetime. The 537.0-Å line excitation ratio shows similar variation with velocity (and  $T_f$ ) to that of the 584.3-Å line, but owing to the higher excitation energy of the  $3^1P$  level and the intermediate levels important in the indirect excitation of the 537.0-Å line, the excitation rate ratio peaks at a slightly higher temperature and falls off more slowly (relative to its absolute magnitude) than for the 584.3-Å line. Very similar calculations to those performed for the 584.3-Å line were carried out. The integrated intensity enhancement factors computed for the 537.0-Å line are 14 (EMD S) and 27 (EMD X) for  $P_e = 6 \times 10^{14} \text{ cm}^{-3}$  K, and 22 (S) and 26 (X) for  $P_e = 2 \times 10^{14} \text{ cm}^{-3}$  K. The trends exhibited are the same as those seen in the calculations for the 584.3-Å line. The ratio of the enhancements computed for the two He I lines is discussed in Section 4.

### 3.3 Non-Maxwellian effects

Many studies of the electron velocity distribution function (EVDF) in the solar transition region have suggested that significant departures from a Maxwellian distribution may occur (e.g. Shoub 1983; Ljepojevic & Burgess 1990; Viñas,

Wong & Klimas 2000). This could be due to streaming of fast electrons from the high TR and corona down the steep temperature gradient or due to accelerating processes in the chromosphere or transition region. A form of the EVDF appropriate to the former process has been used an extensive investigation of the effects of such a distribution on the helium spectrum (Paper II). Here we briefly consider the effects of that non-Maxwellian EVDF on the enhancements predicted by the turbulent transport calculations.

An EVDF that is Maxwellian below a cut off velocity of 3.5 times the thermal velocity,  $\sqrt{2kT_e/m}$ , with a power law decline with  $v^{-31/7}$  (Shoub 1982) at higher velocities was considered. This represents a particularly large departure from the Maxwellian form, and was chosen in order to produce the maximum effect on collision rates (Smith 2000). A quantitative investigation of the effects of such a distribution on collision rates (and hence on ground state mean lifetimes) was performed by comparing excitation and ionization rates computed in radiative transfer calculations with and without the non-Maxwellian tail.

This comparison showed that the power law tail in the non-Maxwellian distribution function does not have a significant effect on the collision rates at temperatures much above the normal peak temperature of formation ( $T_i$ ). At higher temperatures the excitation energies of the helium resonance lines correspond to the energies of electrons in the Maxwellian part of the local distribution, and these electrons dominate the excitation rates. At and below  $T_i$ , collisional excitation and ionization occurs predominantly by electrons in the suprathermal tail of the distribution, and so rates are significantly enhanced compared with the Maxwellian case. In the enhancement process investigated here, as excitation occurs mainly at temperatures much higher than  $T_i$ , the power law tail has little effect except at  $T_i$ . The principal effect is to reduce the mean lifetime of the He I and He II ground states at their respective  $T_i$ . For He II this effect is minimal, reducing  $\tau(T_i)$  by 10 per cent, but for He I the reduction is more significant, being by a factor of about 7.

The increase in  $C_{ij}(T_i)$  in equation (5) would also tend to reduce the computed enhancement factor, simply because emission at  $T_i$  would be increased; the effect would not be related to the efficiency of turbulent transport. The change in  $C_{ij}(T_i)$  is therefore ignored in assessing the effects of the non-Maxwellian EVDF on the enhancement factor.

The decrease of  $\tau(T_i)$  has negligible effect on the enhancements computed for the He II line, but noticeable effects on those computed for the He I lines. Excitation of the 584.3-Å and 537.0-Å lines occurs mainly at the same temperatures and heights as in the calculations with Maxwellian excitation, but the velocities required by plasma elements to reach those heights are greater. There is, therefore, some reduction of the total enhancement (the same effect occurs for He II, but to a very much smaller extent). The reduction is relatively greater in the case of EMD S (the enhancement factor is smaller by about 30 per cent) than for EMD X, as the temperature gradient above  $\log T_e = 4.5$  is smaller in the former case. The velocity required to reach a particular temperature is increased for EMD S by a greater amount relative to  $\sqrt{\langle v_i^2 \rangle(T_i)}$  than for EMD X, reducing the Gaussian weighting  $G(v)$  to a greater extent in calculating the EMD S enhancement factor.

In the 537.0-Å line, the effect of the smaller  $G(v)$  at high

**Table 3.** Upper limits on intensity enhancement factors for the helium lines calculated for EMDs S and X. An assumed pressure of  $P_e = 2 \times 10^{14} \text{ cm}^{-3} \text{ K}$  is denoted by (a),  $P_e = 6 \times 10^{14} \text{ cm}^{-3} \text{ K}$  is denoted by (b).

Ion	Wavelength (Å)	Enhancement factor			
		S(a)	X(a)	S(b)	X(b)
He II	303.8	6.9	7.0	5.3	5.5
He I	584.3	15.3	17.6	11.2	18.7
He I	537.0	22.4	26.0	14.1	26.5

temperatures leads to a reduction in the temperature of the peak intensity enhancement so that it occurs in the same region as for the 584.3-Å line. This would tend to reduce any variation in the ratio of intensities of the two lines compared with the case in which Maxwellian excitation is assumed. The enhancement of the 537.0-Å line is also decreased, by almost a factor of two in calculations with EMD S, but by a much smaller amount in the case of EMD X.

## 4 DISCUSSION AND CONCLUSIONS

The intensity enhancement factors calculated for the helium resonance lines in the presence of turbulent transport are given in Table 3. As discussed above, these should be regarded as upper limits. In the case of He II the over-estimates should be relatively small, and an intensity enhancement of approximately a factor of 5 is plausible, given the parameters assumed to describe the solar atmosphere. This is similar to the factors predicted by Jordan (1980) and Andretta et al. (2000) using a less satisfactory expression for the excitation time. An enhancement factor of 5 cannot account entirely for the enhancement of at least a factor of 13 apparently required in the network according to the analysis of MJ99. However, using the current second order correction of *sim25* for the NIS 2 waveband of CDS instead of the factor of 55 derived by Landi et al. (1997), the required enhancement is only a factor of 6 (as found by Jordan 1975), which is within the range calculated here. Radiative transfer calculations (Smith 2000) using the VAL (Vernazza et al. 1981) models of the quiet solar atmosphere under-produce the 303.8-Å line intensity by factors of 3–4, which the present work shows could be explained entirely by the enhancement mechanism suggested here.

The enhancement factors derived for the He I 584.3-Å line are also upper limits, but show that enhancement factors of order 10 are plausible. Thus non-thermal transport of He I could produce the enhancement of the resonance line intensity required to account for the results of MJ99.

Calculations of the 584.3-Å line intensity using the VAL C (average quiet Sun) and VAL D (average network) models produce fairly good matches to observations (Andretta & Jones 1997; Smith 2000), but produce too much emission in other low transition region lines, owing to the presence of the temperature plateau at  $T_e \simeq 2.5 \times 10^4 \text{ K}$ . However, models of the atmosphere in which the plateau is removed do not produce high enough intensities in the He I line to match the observations, but by smaller factors than required by MJ99

(Andretta & Jones 1997; Smith 2000). These discrepancies could also be explained by the factors found here.

Similar arguments hold for the He I 537.0-Å line, for which an enhancement of a factor of up to about 25 is predicted by the calculations presented here. It is interesting that greater enhancement factors are predicted for the 537.0-Å line than for the 584.3-Å line, as radiative transfer calculations using the VAL models (Andretta & Jones 1997; Smith 2000) show the predicted ratio  $I(537.0 \text{ \AA})/I(584.3 \text{ \AA})$  to be smaller than observed. MJ99 found a ratio of  $0.116 \pm 0.015$  in the network (using the Landi et al. 1997 calibration of CDS;  $0.105 \pm 0.014$  using the Brekke et al. 2000 calibration), but calculations using the VAL models give values of about 0.08. Enhancements of the two lines in the ratio derived here would help resolve this disagreement. Radiative transfer calculations using a model atmosphere based on EMD S produce a value of 0.117 (Paper II); the enhancements predicted here would therefore worsen agreement with observations. Nevertheless, the enhancement factors calculated here give an intensity ratio much closer to that observed than do radiative transfer calculations of the effects of non-local suprathermal electrons which produce enhancement factors of the same order (Paper II).

In the formulation used here, the efficiency of the non-thermal transport process increases with decreasing pressure. For example, the predicted 303.8-Å and 584.3-Å line intensity enhancements are increased by about 30 per cent when the pressure is reduced by a factor of 3. This would appear to conflict with observations of coronal holes, where electron pressures are lower than in the quiet Sun by factors of 2 – 3 (Munro & Withbroe 1972; Jordan et al. 2001), but where helium line intensities (and required enhancements) are smaller. However, the energy balance adopted here in the upper TR (equation (10)) takes no account of the fast solar wind and the term in  $A(r)$  does not allow for super-radial expansion. For non-thermal transport calculations appropriate to coronal holes, energy balance calculations specifically for coronal holes are required; these could be combined with observed EMDs in a similar manner to that described here. Further observations of the helium lines in coronal holes on the disk would be useful (to avoid the problems of limb darkening/brightening seen in polar coronal holes). It would also be interesting to investigate non-thermal transport in active regions (for which Andretta et al. 2000 predict smaller enhancements), where electron pressures are higher and turbulent velocities lower than in the quiet Sun.

Turbulent transport could help explain the spatial variations of the intensities of the helium lines with respect to each other and to other TR lines in the quiet Sun. The increases in the heights of peak line formation predicted here are not large enough to be resolved directly at the limb, but the effects of the increased *temperatures* of emission may perhaps be seen in observations of the network, the appearance of which changes between the low and high TR. The turbulent motions of the largely ionized gas would be influenced by the direction of the network field, so that material moving to greater heights would trace the expansion of the network (see e.g. Gabriel 1976). The width and the contrast of the network observed in the He I and He II lines seem to resemble that seen in high TR lines like those of Ne VI ( $\log T_e = 5.6$ ) and Ne VII ( $\log T_e = 5.7$ ), rather than that seen in lower TR lines of C II ( $\log T_e = 4.4$ ), C III (4.9),

or even O III (5.05), O IV (5.25) or O V (5.4) (Brueckner & Bartoe 1974; Withbroe 1976; Gallagher et al. 1998; Patsourakos et al. 1999). Patsourakos et al. (1999) found that Gabriel's (1976) model predicts a network width which increases with temperature, reaching the width observed in helium at  $\log T_e \simeq 5.75$ . The present calculations predict He I emission to peak at  $\log T_e \simeq 5.2$ , and He II emission to peak at  $\log T_e \simeq 5.3$ , but with significant contributions in each case from temperatures up to  $\log T_e \simeq 5.6$ . There is little contribution to intensity above  $\log T_e \simeq 5.7$ , but the calculations assume different pressures and temperature gradients (and overall geometry) to those in the Gabriel (1976) model, making quantitative comparisons difficult. Qualitatively, however, turbulent transport in an expanding network could explain why the pattern of helium emission resembles that seen in lines formed in equilibrium at higher temperatures and heights. In a similar geometry, suprathermal electrons streaming down the field lines from the upper TR would be expected to be funnelled into the network in the low TR, which would concentrate any enhanced helium emission in the centre of the network, which would be less consistent with the observed width of the network.

Turbulent transport of helium in an expanding network is also qualitatively consistent with observed variations in the ratio of the intensities of the He I lines,  $I(537.0 \text{ \AA})/I(584.3 \text{ \AA})$ . The excitation rate ratio for the 537.0-Å line peaks at a slightly higher temperature and falls off more slowly at higher temperatures than for the 584.3-Å line. This suggests that the network could appear wider in the 537.0-Å line than in the 584.3-Å line, which is broadly consistent with rastered images in the two lines (MJ99), although further observations of the two lines would be useful. The ratio  $I(537.0 \text{ \AA})/I(584.3 \text{ \AA})$  would be expected to increase towards the edges of the network, but the variation would be relatively small, since the ratio of the enhancement factors of the two lines changes by only 25 per cent between  $\log T_e = 4.8$  and  $\log T_e = 5.7$ . This factor is consistent with values of the ratio observed by MJ99, who found only small variations of the ratio, but a consistent increase in the ratio in regions of smaller absolute intensity. Enhanced excitation by non-local suprathermal electrons in the low TR would tend to produce a larger variation in the opposite sense with absolute intensities (Paper II).

In a more refined approach to turbulent transport calculations, improvements could be made to the simple geometry adopted here. Flux tubes with various inclinations could be modelled, allowing a more quantitative examination of how the spatial variation of helium emission may be affected. MJ99 found steeper temperature gradients in cell interiors than in the network, but these gradients may be *across* magnetic structures. In the expanding network picture, the temperature gradient *along the field* is smaller, which would reduce the enhancement factor, as would the higher pressures found by MJ99 in cell interiors. The greater helium line enhancements required by MJ99's observations in cell interiors could possibly be caused by photon scattering from the boundaries; radiative transfer using two-component model atmospheres is needed to test this point.

As described in Section 3.3, even significantly non-Maxwellian EVDFs are expected to have relatively little effect on turbulent transport of helium in the quiet Sun. As enhancements of the helium line intensities by non-thermal

motions occur at temperatures much higher than the normal temperature of peak line formation, and enhancement by non-local suprathermal electrons occurs largely at lower temperatures (Paper II), the two processes could be operating simultaneously. If non-thermal motions do produce the enhancement factors calculated here, these would dominate over the effects of non-local electrons, provided departures from Maxwellian EVDFs are realistic (Paper II).

The present calculations do not include radiative transfer, which could have significant effects on He I, but which would be less important for He II. Radiative transfer calculations including non-thermal motions (and possibly non-Maxwellian EVDFs as well) are needed to place our conclusions on a firmer footing.

## ACKNOWLEDGMENTS

GRS acknowledges the financial support of PPARC as a DPhil student, under grant PPA/S/S/1997/02515.

## REFERENCES

- Aggarwal K. M., 1993, *ApJS*, 85, 197
- Aggarwal K. M., Callaway J., Kingston A. E., Unnikrishnan K., 1992, *ApJS*, 80, 473
- Anderson S. W., Raymond J. C., Ballegoijen A. V., 1996, *ApJ*, 457, 939
- Andretta V., Jones H. P., 1997, *ApJ*, 489, 375
- Andretta V., Landi E., Del Zanna G., Jordan S. D., 1999, in Vial J.-C., Kaldeich-Schürmann B., eds, *Proc. 8th SOHO Workshop, ESA SP-446, Plasma Dynamics and Diagnostics in the Solar Transition Region and Corona*. ESA Publications Division, Noordwijk, p. 123
- Andretta V., Jordan S. D., Brosius J. W., Davila J. M., Thomas R. J., Behring W. E., Thompson W. T., Garcia A., 2000, *ApJ*, 535, 438
- Arnaud M., Rothenflug R., 1985, *A&AS*, 60, 425
- Avrett E. H., 1999, in Vial J.-C., Kaldeich-Schürmann B., eds, *Proc. 8th SOHO Workshop, ESA SP-446, Plasma Dynamics and Diagnostics in the Solar Transition Region and Corona*. ESA Publications Division, Noordwijk, p. 141
- Berger R. A., Bruner E. C., Jr., Stevens R. J., 1970, *Solar Phys.*, 12, 370
- Boland B. C., Engstrom S. F. T., Jones B. B., Wilson R., 1973, *A&A*, 22, 161
- Brekke P., Thompson W. T., Woods T. N., Eparvier F. G., 2000, *ApJ*, 536, 959
- Brueckner G. E., Bartoe J.-D. F., 1974, *Solar Phys.*, 38, 133
- Capelli A., Cerutti-Sola M., Cheng C., Pallavicini R., 1989, *A&A*, 213, 226
- Chae J., Schühle U., Lemaire P., 1998, *ApJ*, 505, 957
- Doschek G. A., Feldman U., VanHoosier M. E., Bartoe J.-D. F., 1976, *ApJS*, 31, 417
- Drake G. W. F., 1996, in Drake G. W. F., ed., *Atomic, Molecular & Optical Physics Handbook*. AIP Press, p. 154
- Fontenla J. M., Avrett E. H., Loeser R., 1993, *ApJ*, 406, 319
- Gabriel A. H., 1976, *Phil. Trans. R. Soc. Lond.*, A 281, 339
- Gallagher P. T., Phillips K. J. H., Harra-Murnion L. K., Keenan F. P., 1998, *A&A*, 335, 733
- Hammer R., 1997, in Wilson A., ed., *5th SOHO Workshop, ESA SP-404, The Corona and Solar Wind Near Minimum Activity*. ESA Publications Division, Noordwijk, p. 141
- Hearn A. G., 1969, *MNRAS*, 142, 53
- Jordan C., 1975, *MNRAS*, 170, 429
- Jordan C., 1980, *Phil. Trans. R. Soc. Lond.*, A 297, 541
- Jordan C., 1991, in Ulmschneider P., Priest E. R., Rosner R., eds, *Mechanisms of Chromospheric and Coronal Heating*. Springer-Verlag, Berlin, p. 300
- Jordan C., 2000, *Plasma Phys. Control. Fusion*, 42, 415
- Jordan C., Brown A., 1981, in Bonnet R. M., Dupree A. K., eds, *Solar Phenomena in Stars and Stellar Systems*. Reidel, Dordrecht, p. 199
- Jordan C., Ayres T. R., Brown A., Linsky J. L., Simon T., 1987, *MNRAS*, 225, 903
- Jordan C., Macpherson K. P., Smith G. R., 2001, *MNRAS*, 328, 1098
- Landi E., Landini M., Pike C. D., Mason H. E., 1997, *Solar Phys.*, 175, 553
- Landini M., Landi E., 1998, *A&A*, 340, 265
- Lanzafame A. C., Tully J. A., Berrington K. A., Dufton P. L., Byrne P. B., Burgess A., 1993, *MNRAS*, 264, 402
- Ljepojevic N. N., Burgess A., 1990, *Proc. R. Soc.*, A 428, 71
- Macpherson K. P., Jordan C., 1999, *MNRAS*, 308, 510
- Mariska J. T., 1992, *The Solar Transition Region*. CUP
- Mihalas D., Stone M. E., 1968, *ApJ*, 151, 293
- Milkey R. W., 1975, *ApJ*, 199, L131
- Munroe R. H., Withbroe G. L., 1972, *ApJ*, 176, 511
- Patsourakos S., Vial J.-C., Gabriel A. H., and Bellamine N., 1999, in Vial J.-C., Kaldeich-Schürmann B., eds, *Proc. 8th SOHO Workshop, ESA SP-446, Plasma Dynamics and Diagnostics in the Solar Transition Region and Corona*. ESA Publications Division, Noordwijk, p. 537
- Peter H., 1999, *ApJ*, 522, L77
- Peter H., 2001, *A&A*, 374, 1108
- Philippides D., 1996, DPhil Thesis, University of Oxford
- Rutten R. G. M., Schrijver C. J., Lemmens A. F. P., Zwaan C., 1991, *A&A*, 252, 203
- Sawey P. M. J., Berrington K. A., 1993, *A.D.N.D.T.*, 55, 81
- Shoub E. C., 1982, *Stanford University Institute for Plasma Research, Report No. 946*
- Shoub E. C., 1983, *ApJ*, 266, 339
- Sim S. A., Jordan C., 2001, in Favata F., Drake J., eds, *ASP Conf. Ser. Vol. TBD, Stellar Coronae in the Chandra and XMM-Newton Era*. Astron. Soc. Pac., San Francisco, in press
- Smith G. R., 2000, DPhil Thesis, University of Oxford
- Spitzer L., 1956, *Physics of Fully Ionized Gases*. Interscience, New York
- Tousey R., 1967, *ApJ*, 149, 239
- Vernazza J. E., Avrett E. H., Loeser R., 1981, *ApJS*, 45, 635
- Viñas A. F., Wong H. K., Klimas A. J., 2000, *ApJ*, 528, 509
- Wahlström C., Carlsson M., 1994, *ApJ*, 433, 417
- Withbroe G. L., 1976, in Bonnet R. M., Delache P., eds, *Proc. IAU Colloq. no. 36, The Energy Balance and Hydrodynamics of the Solar Chromosphere and Corona*. p. 263
- Zirin H., 1975, *ApJ*, 199, L63